Evaluation of Fungal Deterioration in *Liquidambar orientalis* Mill. Heartwood by FT-IR and Light Microscopy

Nural Yilgor,[a,*] Dilek Dogu,[b] Roderquita Moore,[c] Evren Terzi,[b] and S. Nami Kartal [b]

The chemical and morphological changes in heartwood specimens of *Liquidambar orientalis* Mill. caused by the white-rot fungus *Trametes versicolor* and the brown-rot fungi *Tyromyces palustris* and *Gloeophyllum trabeum* were studied by wet chemistry, FT-IR, GC-MS analyses, and photo-microscopy. According to GC-MS results, 26 extracts identified in the ethanol/toluene extraction and 17 in the ethanol extraction were found. Heartwood specimens of *L. orientalis* were highly susceptible to the fungi tested. While 1% NaOH solubility increased 35% in the specimen decayed by *T. palustris*, only an 8% increase was seen in the specimen exposed to *T. versicolor* when compared to the control specimen. Decayed wood by *T. palustris* showed a 5.5% increase in the Klason lignin content when compared to control specimens; however, the Klason lignin content decreased after a *T. versicolor* attack for 12 weeks. A *T. versicolor* attack in the cell walls was seen both from the lumina and from the cell corners, and the attack from the cell corners was mainly clear in ray parenchyma cells. An excessive destruction was detected in the wood structure attacked by *T. palustris*. The cell collapse was caused by a distortion in the plane of the wood cells. This extensive degradation was seen in all types of cell walls. Cracks in the cell walls were also detected in the specimens.

Keywords: Fungal degradation; GC-MS; Extractives; Morphology of wood decay; FT-IR; Liquidambar orientalis

*Contact information: a: Department of Forest Products Chemistry and Technology, Forestry Faculty, Istanbul University, 34473, Istanbul, TURKEY; b: Department of Forest Biology and Wood Protection Technology, Forestry Faculty, Istanbul University, 34473, Istanbul, TURKEY; c: USDA Forest Service, Forest Products Laboratory, Madison, WI, 53726, USA; *Corresponding author: yilgorn@istanbul.edu.tr*

INTRODUCTION

Wood is a natural, renewable, and valuable construction material. Since being thought of as naturally resistant to wood-degrading organisms, wood has often been used as a shelter, and has many outdoor applications throughout human history. However, the durability of wood varies depending on its tree species, chemical composition, and the environmental conditions the wood is exposed to. Wood biodegradation occurs in different ways such as fungal, bacterial, and insect attack. Fungal decay is the most widespread type of wood degradation, and wood decay fungi are usually classified in three main groups: white, soft, and brown-rot (Eriksson *et al*. 1990; Blanchette 1995). Of

these, only white-rot fungi are capable of degrading the hemicelluloses, cellulose, and lignin, whereas soft-rot fungi can degrade cellulose and hemicellulose and partially digest lignin. Brown-rot fungi are not able to digest lignin while they decompose the hemicelluloses and cellulose (Erikkson *et al*. 1990; Blanchette 1995).

The development of new techniques has provided a great deal of understanding about the mechanism of fungal degradation of wood polymers, but there are still many questions that remain unanswered regarding wood biodegradation by fungi (Hatakka and Hammel 2010).

In this study, *Liquidambar orientalis,* one of the most important endemic hard-wood species in Turkish flora, was investigated with respect to some of its chemical and anatomical properties after being exposed to the white- and brown-rot fungi. In recent years, various projects regarding protection of *L. orientalis* trees, development of new plantations, and realization of new management plans for balsam production have been started in Turkey due to the usage of its wood for indoor building and roofing material as well as balsam production (Terzi *et al.* 2012). The influence of fungal degradation on both gymnosperm and angiosperm wood species in terms of anatomical and chemical changes have been studied. Flournoy *et al*. (1991) examined the mechanism of cellulose depolymerization in sweetgum (*L. styraciflua* L.) wood specimens exposed to brown-rot fungus, *Postia placenta*. Highley and Murmanis (1987) studied micro-morphological changes in sweetgum and western hemlock sawdust caused by white-rot fungus, *Trametes versicolor*. However, many of the wood species and the degradation caused by fungi have become an interest for many researchers after the development of new instrumental techniques such as FT-IR, GC-MS, NMR, *etc*. Of these, FT-IR is one of the most useful and valuable tools for investigating fungal decay and has been used to observe the effects of fungi in wood structures. It is also useful to characterize the chemical changes in the molecular structure of woods exposed to biological attacks such as fungal and bacterial. Faix *et al.* (1991) examined beech wood attacked by white-rot fungus by FT-IR spectroscopy and analytical pyrolysis; results indicated that lignin was modified more than polysaccharides. Pandey and Pitman (2003) studied *Pinus sylvestris* L. sapwood and *Fagus sylvatica* L. wood specimens by FT-IR after different exposure periods by brown and white rot fungi. Another study by Pandey and Pitman (2004) examined the lignin content of both softwood and hardwood after decay by brown rot fungus with FT-IR. Naumann *et al*. (2005) demonstrated that FT-IR technology has an ability to identify wood fungi, and it is possible to detect fungi in wood by FT-IR microscopy. Rumana *et al*. (2010) used FT-IR spectroscopy to characterize the lignin structure, and five tropical timber wood species of the family of Dipterocarpaceae were investigated with regard to chemical and histochemical properties. FT-IR spectroscopy, on the other hand, requires the preparation of small pellets with KBr which might be time consuming and tedious. In recent years, a new technique called "Attenuated Total Reflectance" (ATR) has been developed and used in conjunction with infrared spectroscopy. Mohebby (2005) studied beech wood that had been exposed to a white rot fungus for a period 84 days with ATR spectroscopy by means of chemical alteration of the wood structure. The study claimed that ATR spectroscopy was a very feasible and rapid method for examining biodegradation caused by fungi in wood.

The goal of this study was to identify some of the chemical components of *L. orientalis* heartwood by GC-MS and monitor the changes in wood structure after brown and white fungi exposure by means of FT-IR ATR spectroscopy and light microscopy.

EXPERIMENTAL

Decayed Wood Specimens

Details regarding heartwood specimens and decay tests are given in our previous study (Terzi *et al.* 2012). Soil block decay resistance tests were performed based on the AWPA E10-09 standard method by using 12 replicate heartwood specimens of *L. orientalis* (19 by 19 by 19 mm) for each test fungus. Two brown rot and one white rot fungi (*Tyromyces (Fomitopsis) palustris* (Berkeley and Curtis). Murrill (FFPRI 0507) and *Gloeophyllum trabeum* (Pers:Fries) Murrill, MAD 617 and *Trametes versicolor* (L.: Fr.) Quel. MAD 697 were employed as test fungi (AWPA 2010).

Chemical Analyses

Before chemical analyses, the heartwood and sapwood of *L. orientalis* were separated, and then the air-dry wood specimens were ground and screened through a 40 to 80-mesh sieve according to TAPPI T-257 cm-85 (TAPPI 1992). The ash content of the wood specimens, hot water, and dilute alkali solubility and extractives soluble in solvents were determined according to TAPPI standards T 211 om-93, T 207 om-93, T 212 om-98, and T 204 om- 88, respectively (TAPPI 1999 and 1987).

The Klason lignin content of heartwood was performed based on Runkel and Wilke (1951). The Klason lignin values were corrected for the ash content gravimetrically following the incubation of lignin at 575 °C for less than 3 h.

The carbohydrates content of the hydrolysates was determined by anion exchange high performance liquid chromatography (HPLC) using pulsed amperometric detection (Davis 1998). Wood sugars were quantitated using an internal standard method, and the results were reported in terms of a percentage of the original specimen mass.

In addition, in decayed wood specimens, the Klason lignin content and 1% NaOH solubility were determined using the above standards.

Heartwood Extracts Preparation

To determine the heartwood extractives, ethanol/toluene and ethanol extraction steps were performed according to TAPPI method T 204 om-88 (TAPPI 1987) with slight modifications. The ground wood samples were magnetically stirred with solvents for 48 h. In the first 24 h (2:1) toluene and 95% ethanol were used, and the solvent and extracts were filtered. In the second 24 h, 95% ethanol was used and filtered. The wood extractions had a yellow tint in the solvent. The solvents were dried in the rotary evaporator and the extractives were collected for further investigation by GC-MS.

Gas Chromatography-Mass Spectrometry (GC-MS) Analyses

The extracts were analyzed on a Shimadzu GC-MS-QP2010 instrument (Kyoto, Japan) equipped with split-splitless inlets, a mass spectrometer, and an auto injector. SHRXI-5ms (30m X 0.25 mm I.D., 0.25 μm film thickness) capillary column was used and the carrier gas was helium. The temperature injection was 250 ^{o}C. The oven was temperature-programmed from 50 ^{o}C (1 min) to 320 ^{o}C (10 min) at 10 ^{o}C/min. The National Institute of Standards and Technology (NIST) library was used for identifying components.

FT-IR ATR Spectral Analyses

The IR absorption data were obtained by using a Perkin Elmer 100 FT-IR Spectrometer combined with an ATR unit (Universal ATR Diamond Zn/Se) at a resolution of 4 cm^{-1} for 32 scans in the spectral range 600 to 4000 cm^{-1}. Dried specimens were milled and passed through a mesh 80 sieve, and the analyses were performed on undecayed specimens and specimens exposed to the fungi. The spectra were baseline corrected and normalized to the highest peak. FT-IR spectroscopy was improved by an attenuated total reflectance (ATR) unit that provided direct interaction of the measuring beam with the sample and reflected the attenuated radiation to the spectrometer and increased the sensitivity of FT-IR-based analyses.

Anatomical Examinations

Degraded heartwood specimens were cut directly into thin sections by using a sliding microtome. The sections were then stained with safranin and picro-aniline-blue. A specimen obtained from the heartwood of sound wood served as the control. That sample was kept under vacuum in the presence of alcohol, glycerin, and water at room temperature to soften it before it was sectioned. The sections were only stained by safranin. Evaluations were performed using an Olympus BX51 Light Microscope, and images were taken using analySIS FIVE Software; a DP71 Digital Camera was installed and adapted on the microscope. All of the microscopic investigations and evaluations were realized on cross, radial, and tangential sections.

RESULTS AND DISCUSSION

Chemical Analyses

Table 1 shows the amount of Klason lignin and the monomer sugars in undecayed heartwood specimens of *L. orientalis*. The solubility values by ethanol/toluene, ethanol, hot water, and 1% NaOH are given in Table 2. The ash content of heartwood specimen was determined as 0.42%. Table 3 represents the amount of Klason lignin and hot alkali solubility of the specimens exposed to the brown rot and white rot fungi tested; percentage changes in these values after fungal attack were based on the undecayed specimens. The ethanol/toluene extractable content of the wood consisted of the waxes, fats, resins, oils, and tannin. The hot water extraction removed a part of the extraneous components, such as inorganic compounds, tannins, gums, sugars, coloring matter, and starches. Hot alkali soluble extracts contain low molecular weight carbohydrates and degraded cellulose. Besides undecayed specimens, Klason lignin content and 1% NaOH solubility were determined in the specimen exposed to either *Tyromyces (Fomitopsis) palustris* or *Trametes versicolor*. While alkali solubility was found as 18.7% in the control specimen, it was 25.3% and 20.2% in the specimens exposed to *T. palustris* and *T. versicolor*, respectively. As expected, 1% NaOH solubility remarkably increased in the specimen decayed by *T. palustris* since the brown-rot fungi degraded wood carbohydrates selectively. Even though the high solubility of 1% NaOH indicates the degradation of the hemicelluloses and degraded cellulose in wood, it was 20.2% in the specimen exposed to *T. versicolor* in our study. While 1% NaOH solubility showed a 35.3% increase in the specimen decayed by *T. palustris*, only an 8% increase in the specimen exposed to *T. versicolor* was seen when compared to the control specimen. An increase in alkali solubility is an efficient sign of carbohydrate decomposition, and *T. palustris* caused a

remarkable decomposition in the carbohydrates compared to *T. versicolor* due to high alkali solubility in the study (Table 3). The decayed wood specimens by *T. palustris* showed a 5.5% increase in the Klason lignin content when compared to the control specimen; however, the Klason lignin content decreased after the *T. versicolor* attack for 12 weeks. This might be an indication that the fungus, *T. versicolor*, degraded the lignin part of the wood preferentially.

Table 1. Chemical Properties of Undecayed Heartwood of *L. orientalis*

Klason lignin (%)	Arabinose (%)	Galactose (%)	Rhamnose (%)	Glucose (%)	Xylose (%)	Mannose (%)	Total Carbohydrates (%)
22.63	0.61	0.95	0.42	43.05	20.76	3.18	69.00

All values are average of duplicate analyses.

Table 2. Solubility of Undecayed Heartwood of *L. orientalis*

Solubility	%
Ethanol/toluene solubility	2.73
Ethanol solubility	1.98
Hot water solubility	5.64
1% NaOH solubility	18.72

All values are average of duplicate analyses.

Table 3. Klason Lignin Content, 1% NaOH Solubility, and Percentage Changes in Control and Decayed Wood Specimens

	Klason lignin		1% NaOH solubility	
Specimens	Average (%)	Change (%)*	Average (%)	Change (%)*
Undecayed control	22.63	-	18.72	-
Decayed by *T. palustris*	23.87	+5.5	25.33	+35.3
Decayed by *T. versicolor*	21.27	-6	20.21	+8

* Based on undecayed control specimens. All values are average of duplicate analyses.

The present test results were in good agreement with a study by Winandy and Morrell (1993), who studied the relationship between decay and the chemical composition of Douglas-Fir heartwood, and performed decay tests with *A. placenta* and *G. trabeum* as the brown-rot fungi and *T. versicolor* and *B. adusta* as the white-rot fungi. Their results showed that the brown rot fungi caused more substantial changes in the chemical composition. The alkali solubility of the specimens colonized by the brown-rot fungi gradually increased with longer incubation periods. The Klason lignin content of the specimens colonized by either of the two brown-rot fungi remarkably increased during the 177-day-incubation period. Furthermore, it was suggested that both of the white-rot fungi caused a minimal effect on the chemical properties of the wood, as shown by the alkali solubility.

Mass Loss in Decayed Wood Specimens

Heartwood specimens of *L. orientalis* were susceptible to fungal decay by the two brown-rot fungi and one white-rot fungus tested. Mass losses have been reported for such specimens in decay resistance tests (Terzi *et al*. 2012). *T. palustris* degradation caused around a 50% mass loss in the specimens. Mass losses in the specimens varied between 37% and 43% for the *G. trabeum* attack.

The white-rot fungus *T. versicolor* caused mass losses that varied from 34% to 41%. According to the ASTM D 2017 classification (ASTM 2010), the heartwood specimens of *L. orientalis* were "non-resistant" against the *T. palustris*; however, the specimens were moderately resistant against *G. trabeum* and *T. versicolor* based on the average mass losses (Terzi *et al*. 2012).

GC-MS Analyses

Results from the GC-MS analyses are shown in Figs. 1a and 1b. Compounds having a peak area of 1% or more are given in Table 4. According to the GC-MS results, there were 26 extracts identified in the ethanol/toluene extraction and 17 in the ethanol extraction. Thirty-five was the total number of compounds identified from both extractions. Three replicates of the samples were injected into the GC-MS.

As can be seen in Fig. 1a, 26 compounds were identified by the NIST library in the first extraction step with the solvents ethanol/toluene. Some of the compounds' concentrations were in trace amounts. Compounds 9, 10, 11, and 12 did not have baseline separation; however, they were identified by the NIST library as 2-furancarboxaldehyde, 5-(hydroxymethyl) (9), hydrocinnamic alcohol (10), 2-butanone, 4-phenyl- (11), and benzene, 2-ethenyl-1,3,5-trimethyl-(12). The most abundant compound is benzaldehyde, representing peak 1 in the ethanol/toluene extraction step.

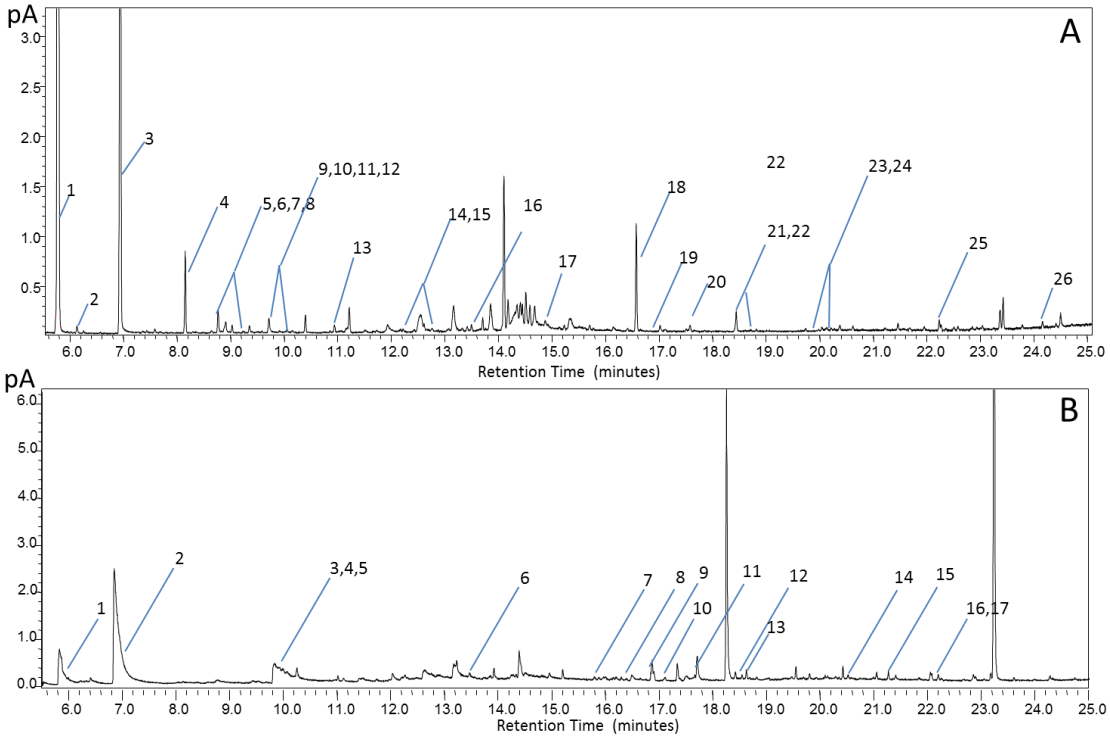

Fig. 1. a) Ethanol/toluene extracts fractionation chromatogram (26 compounds identified by the NIST); b) Ethanol extracts fractionation chromatogram (17 compounds identified by the NIST)

Table 4. Major Chemical Compounds of Ethanol/Toluene and Ethanol Extractions of *L. orientalis* Heartwood by GC-MS Analysis

Compounds	Peak number	Retention time	Peak area (%)
Ethanol/toluene extraction			
Benzaldehyde	1	5.77	65.45
Benzyl alcohol	3	6.94	13.78
Benzyl benzoate	18	16.57	6.36
Benzaldehyde dimethyl acetal	4	8.15	4.52
2-Furancarboxaldehyde, 5-(hydroxymethyl)	9	9.71	1.66
2-Butanone,4-phenyl-	11	9.93	1.10
Ethanol extraction			
Benzyl alcohol	2	6.86	57.03
Benzaldehyde	1	5.84	13.24
2-Furancarboxaldehyde, 5-(hydroxymethyl)	3	9.84	7.59
Salicylic acid	11	17.71	4.08
Hydrocinnamic alcohol	4	9.94	3.77
Tetradecanoic acid	9	16.88	3.08
1-Phenoxypropan-2-ol	5	10.07	1.97
Hexanedioic acid, dioctyl ester (adipic acid)	17	22.06	1.51
Benzyl benzoate	8	16.49	1.21
Hexestrol	7	15.80	1.07
Phenol,2,6-bis(1,1-dimethylethyl)-4-methyl	6	13.47	1.06
Pentadecane	13	18.63	1.00

Refer to Figure 4 for peak numbers.

Figure 1b shows the compounds identified by the NIST library in the second extraction step with ethanol. There were some compounds in trace amounts for this extraction as well. Peaks 3, 4, and 5 were not completely separated; however, they were conclusively identified as 2-furancarboxaldehyde, 5-(hydroxymethyl)-, hydrocinnamic alcohol, and 1-phenoxypropan-2-ol, respectively. In the ethanol extraction, benzyl alcohol was more abundant than benzaldehyde. Peak 2 represents benzyl alcohol and peak 1 represents benzaldehyde. Peaks 13, 14, and 15 are naphthalene peaks. Naphthalene has been reported to be a chemical component of storax (Hafizoglu *et al.* 1996). Further investigations are needed to determine whether the naphthalene peaks are natural components of these extractives or contaminates. Benzaldehyde, benzyl alcohol, hydro-cinnamic alcohol, benzyl benzoate, tetradecanoic acid, salicylic acid, and tritetracontane were identified in both extractions. Some of the chemicals found in both of the extractions have been documented as having contributing factors in biological activities.

Lee *et al.* (2009) investigated benzaldehyde, hydrocinnamic alcohol, and benzyl alcohol for anti-fungal activity. The inhibition rates of benzaldehyde and hydrocinnamic alcohol as individual compounds were 100% and 50.3% at $28x10^{-3}$ mg/mL air

concentration, respectively against *P. cactorum*. Benzyl alcohol showed no fungal activity. This study found 4 out of 8 chemicals in *L. orientalis* heartwood having antifungal activity. Benzyl benzoate is known for showing a high toxicity against insects. Terzi *et al*. (2012) demonstrated in the termite and larvae resistance tests that *L. orientalis* heartwood is resistant against these organisms.

IR Spectroscopy Analyses

Undecayed wood (control)

The IR spectra of undecayed *L. orientalis* heartwood are shown in Fig. 2, and the explanations of the wood peaks can be seen in Table 5. The peaks are defined with reference to Harrington *et al.* 1964; Faix 1991; Pandey and Pitman 2003; and Naumann *et al.* 2005. A strong hydrogen bond (O-H) stretching absorption was seen at 3336 cm^{-1} (1), and the following C-H stretching absorption band was around 2917cm^{-1} (2) (Fig. 2).

The region between 1800 and 600 cm^{-1} is called the "fingerprint region" and many significant and well-defined peaks due to the various functional groups present in wood structure can be observed in this region (Pandey and Pitman 1999; Moheby 2005). It is known that the holocellulose content of hardwood is higher than softwood, and even though it is suggested that the position of the carbonyl peak is in a higher wave number for hardwoods (≥1740) (Pandey 1999), there are different findings which indicate lower wave numbers for carbonyl peaks in hardwoods, such as 1730 cm^{-1} in *Eucalyptus regnans* (Harrington *et al.* 1964), 1724 cm^{-1} in *Fagus sylvatica* (Mohebby 2005), and 1738 cm^{-1} in *F. sylvatica* L. (Pandey and Pitman 2004). However, in our study, strong bands at 1734 cm^{-1} (3) and 1235 cm^{-1} (11) were observed, indicating an unconjugated C=O stretching in xylan. Besides the 1734 cm^{-1} band, the 1235 cm^{-1} band also represented acetyl and carboxyl vibrations in the xylan (Harrington *et al.* 1964). According to Harrington, the other wood fractions' contribution to this band is the lowest when compared to the other bands that represent xylan, such as 1260 cm^{-1}, 1055 cm^{-1}, 1030 cm^{-1}, 990 cm^{-1}, and 895 cm^{-1} (Harrington *et al.* 1964). The peak at 1157cm^{-1} (12) is assigned to the C-O-C vibration in cellulose and hemicellulose.

The peaks observed at 1593 cm^{-1} (5) and 1504 cm^{-1} (6) are characteristic peaks for lignin as seen in Fig. 2. Other than 1734 cm^{-1} (3), absorption bands at 1157 cm^{-1} (12) and 896 cm^{-1} (16), also from the carbohydrates, are accepted as reference peaks for polysaccharides (Pandey and Pitman 2003). It is suggested that while the guaiacyl type of lignin, which is characteristic of softwood lignin, absorbs near 1266-1270 cm^{-1} and 1230 cm^{-1} (Faix 1991; Pandey1999), the syringyl type of lignin, which is characteristic for hardwood lignin, absorbs only at 1230 cm^{-1} (Pandey 1999). Similarly, the band at 1235 cm^{-1} (11) was seen at *L. orientalis* heartwood, but the band at 1265 cm^{-1} representing guaiacyl lignin was not detected in *L. orientalis* heartwood. Nevertheless, hardwood lignin contains guaiacyl moieties but the strong absorption band at 1235 cm^{-1}(11) might have suppressed the band at 1265 cm^{-1} and prevented its appearance (Pandey and Pitman 2003). The peaks in the absorption band at 1372 cm^{-1} (9) and 1324 cm^{-1} (10) are assigned to the C-H deformation in cellulose, the hemicelluloses, and the C-H vibration in cellulose and C_1-O vibration in syringyl derivatives, respectively (Pandey and Pitman 2003; Faix 1991). The band near 830 cm^{-1} (17) observed in *L. orientalis* heartwood is referred to as syringyl linkage which represents the hardwood lignin (Higgins *et al.* 1961; Harrington *et al*. 1964).

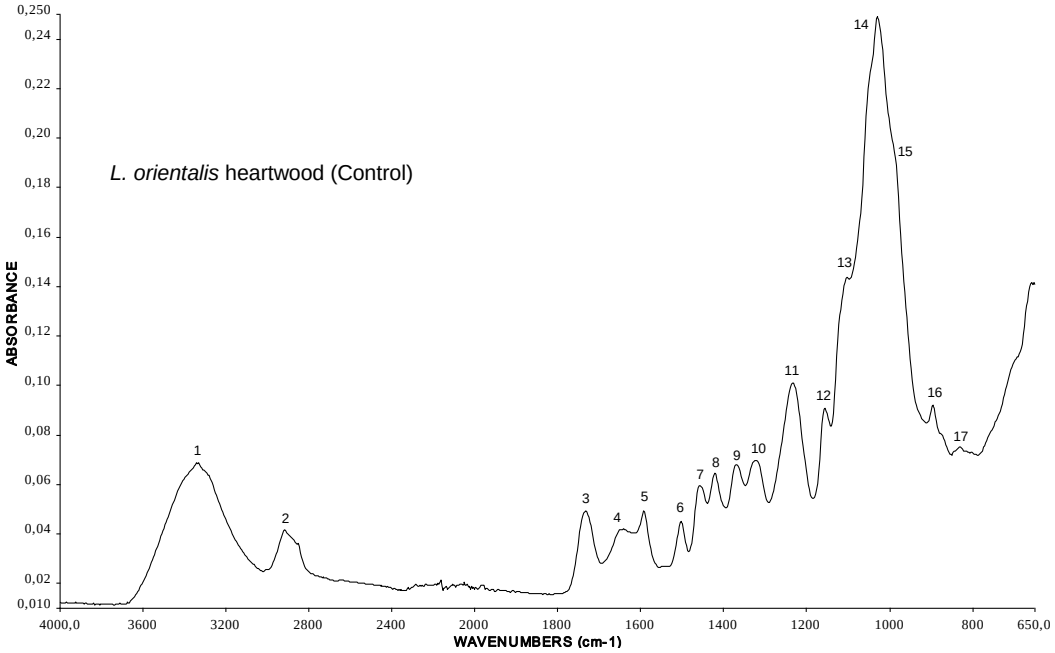

Fig. 2. IR spectrum bands of *L. orientalis* heartwood (control)

Table 5. Assignment of IR Bands

Peak number	Wave number (cm^{-1})	Assignment
1	3336	O-H stretching of bonded hydroxyl groups (1, 2)
2	2917	C-H stretching vibration (2)
3	1734	C=O stretching in xylans (unconjugated) (2,3)
4	1648	H-O-H deformation vibration of absorbed water and C=O stretching in lignin (2)
5	1593	Aromatic skeletal vibrations + C=O stretching S≥ G (3)
6	1504	Aromatic skeletal vibrations in lignin (3,4)
7	1456	CH_2 deformation vibrations in lignin and xylan (2)
8	1422	Aromatic skeletal vibrations combined with C-H in plane deformation + C-H deformation in lignin and carbohydrates (3, 4)
9	1372	C-H deformation in cellulose and hemicellulose (1,4)
10	1324	C-H vibration in cellulose + C_1-O vibration in syringyl derivatives (1)
11	1235	Acetyl and carboxyl vibrations in xylan and C=O stretching vibrations in lignin (2)
12	1157	C-O-C vibration in cellulose and hemicellulose (1,2)
13	1106	O-H association band in cellulose and hemicelluloses (2)
14	1030	C=O stretching vibration in cellulose, hemicelluloses and lignin (2)
15	986	C=O stretching vibration in cellulose and hemicellulose (2)
16	896	C-H deformation in cellulose (1,4)
17	830	Syringyl derivatives representing hardwood lignin (2)

Some of the bands of the spectra in this work slightly differ from literature values. Numbers in parenthesis show the references.
1: Pandey and Pitman 2003; 2: Harrington *et al.* 1964; 3: Faix 1991; 4: Naumann *et al.* 2005

Wood Decayed by *T. palustris* and *G. trabeum*

The IR spectra of *L. orientalis* heartwood exposed to either *T. palustris* or *G. trabeum* for 12 weeks compared to the control specimen are shown in Fig. 3a. It is obvious that the IR spectrum bands of these two brown rot fungi overlap each other except for the spectrum band at 1106 cm^{-1} (13) (Fig. 3a). Actually, the band at 1106 cm^{-1} (13) at the control specimen shifted to 1117 cm^{-1} and 1110 cm^{-1} after deterioration by *T. palustris* and *G. trabeum*, respectively. The shifting of *T. palustris*-spectrums was greater than that of *G. trabeum* compared to the control specimen spectrum (Fig. 3a). According to Harrington *et al.* (1964), the band near 1110 cm^{-1} is assigned to an associated OH bending band on the basis of its response to deuteration in cellulose (Higgins *et al*. 1961; Harrington *et al.* 1964). It is clear that both fungi modified the cellulose, since the spectrum at 1106 cm^{-1} (13) showed an important change when compared to the control specimen (Fig. 3a). Since the spectrums of both brown-rot fungi showed a big similarity and the IR spectrum peaks overlapped, except the band at 1106 cm^{-1} (13), only the spectral peaks of the fingerprint region for *T. palustris* were evaluated along with the control specimen for the fingerprint region (Fig. 3b). As can be seen in Fig. 3b, the absorption peak at 1734 cm^{-1} (3) assigned to a carbonyl group in xylan decreased in the specimen degraded by *T. palustris* when compared to the control specimen. Besides the absorption band at 1734 cm^{-1} (3), a decrease in the absorbance spectrum at 1372 cm^{-1} (9) for the C-H deformation in cellulose and hemicellulose was observed, causing more intensity in the following band at 1324 cm^{-1} (10) from lignin. Even though a 1324 cm^{-1} absorption band was also assigned to the C-H vibration in cellulose, the increase in the intensity of this band indicated that syringyl units were not degraded, and as expected *T. palustris* degradation in the carbohydrates took place selectively. A decrease in the intensity in the spectrum band at 1648 cm^{-1} (4) in the specimen exposed to *T. palustris* was observed, causing an increase in the intensity of the spectrum band at 1593 cm^{-1} (5). The peak at 1648 cm^{-1} (4) was assigned to the H-O-H deformation vibration of absorbed water, and also the region of 1650 to 1600 cm^{-1} could be assigned to conjugated/aromatic carbonyl groups and aromatic rings (Harrington *et al.* 1964; Nuopponen *et al.* 2006). Besides the strong absorption band observed at 1235 cm^{-1} (11) in the control specimen, a shoulder at 1265 cm^{-1} was also detected; this is typical for guaiacyl lignin in the specimen degraded by *T. palustris* (Fig. 3b). Even though the test wood is a hardwood specimen; the shoulder observed at 1265 cm^{-1} in the specimens degraded by the brown rot fungi may be caused by the content of guaiacyl moieties which remain unaffected while the decrease in the intensities of 1235 cm^{-1} (11) band is due to the degradation of xylan (Pandey and Pitman 2003). The intensity at 1157 cm^{-1} (12) representing the carbo-hydrates also decreased in the specimens degraded by brown-rot fungi, as can be seen in Fig. 3b. As expected, the intensity of the carbohydrate band at 896 cm^{-1} (16) was nearly lost when compared to the control specimen. These results were in good agreement with the results by Faix *et al.* 1991 and Pandey and Pitman 2003.

According to ATR spectroscopy results, after 12 weeks of exposure to the brown rot fungi, a significant decrease in the intensity at 1734 cm^{-1} (3), 1372 cm^{-1} (9), 1157 cm^{-1} (12), and 896 cm^{-1} (16) from the polysaccharides occurred. Besides the severe decrease in the intensity of polysaccharide bands, an increase in the intensity of absorption bands at 1593 cm^{-1} (5) and 1504 cm^{-1} (6) was observed, indicating the presence of lignin. It was clear that both brown rot fungi, *T. palustris* and *G. trabeum*, caused a selective degradation in the polysaccharide composition of the wood structure, and this was indicated in a relative increase in the intensities of the lignin bands. Additionally, some of

the peaks shifted in the specimen degraded by *T. palustris*. The band at 1235 cm^{-1} (11) shifted to 1221 cm^{-1} and the band at 1106 cm^{-1} (13) shifted to 1117 cm^{-1} in the degraded specimen when compared to the control specimen (Fig. 3b). Moreover, while the band at 1106 cm^{-1} (13) was a shoulder in the control specimen, it became a remarkable peak after the brown rot fungi degradation, as is clearly apparent in Fig. 3b. Another interesting result concerned the band at 1235 cm^{-1} (11), which shifted and decreased in intensity. This indicated the degradation of xylan and the modification of lignin because this band showed both C-O vibration of acetyl groups in xylan and also the presence of the syringyl type of lignin (Pandey and Pitman 2003). These findings were compatible with the Klason lignin and hot alkali solubility results obtained from the specimen exposed to the brown rot fungi (Table 3).

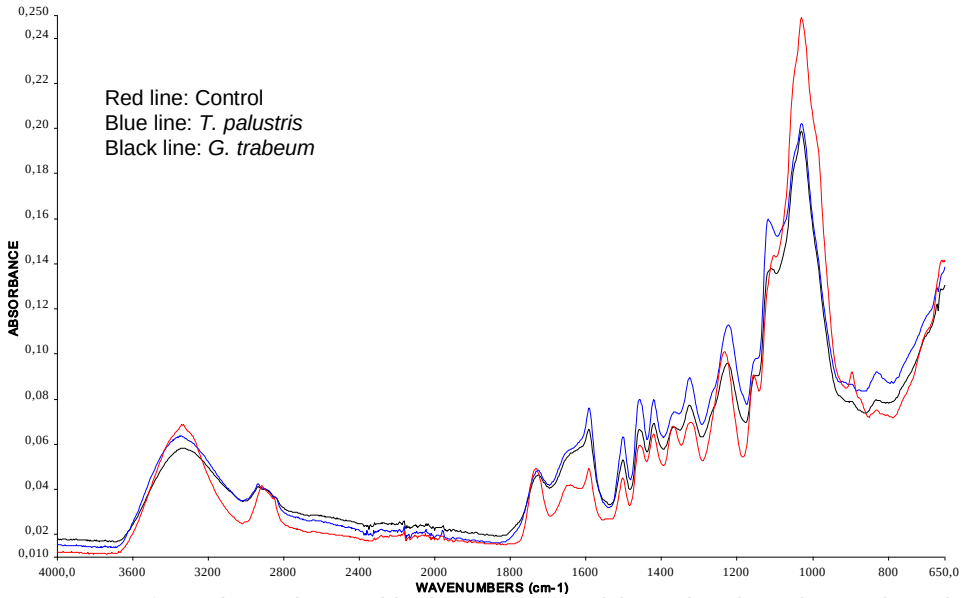

Fig. 3a. IR spectra of specimen decayed by brown-rot fungi (*T. palustris* and *G. trabeum*) and control specimen

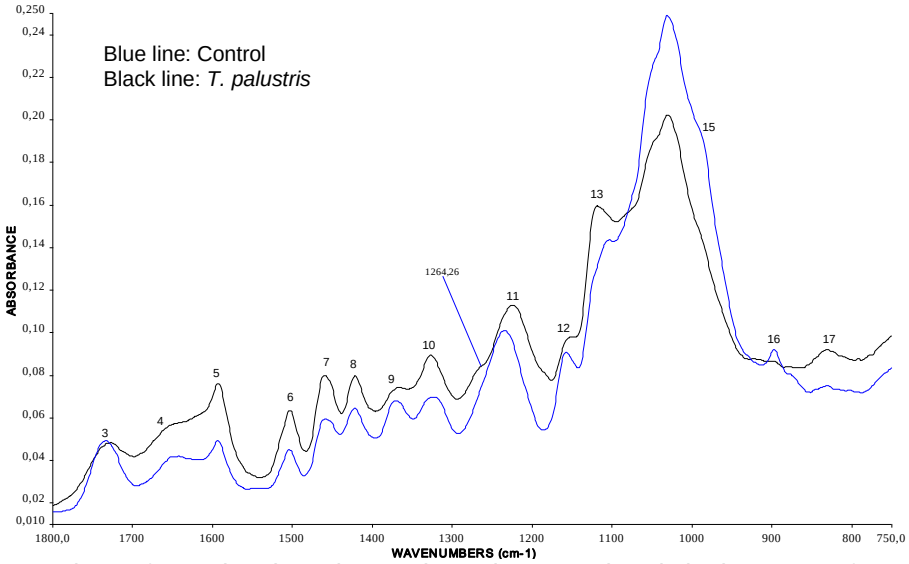

Fig. 3b. Comparison of *T. palustris* and control specimens IR bands in the range of 1800 and 750 cm^{-1}

Wood Decayed by *T. versicolor*

Figure 4a shows FT-IR spectra of the control specimen and the specimen exposed to *T. versicolor*. Unlike the brown-rot fungi (*T. palustris* and *G. trabeum*), no significant change was observed in the specimens degraded by *T. versicolor* in the carbonyl absorption peak at 1734 cm^{-1} (3), which characterizes unconjugated C=O stretching in xylan. Significant decreases were observed in the intensities of the bands at 1593 cm^{-1} (5) and 1504 cm^{-1} (6) which originate from conjugated carbonyl groups in lignin (Fig. 4b).

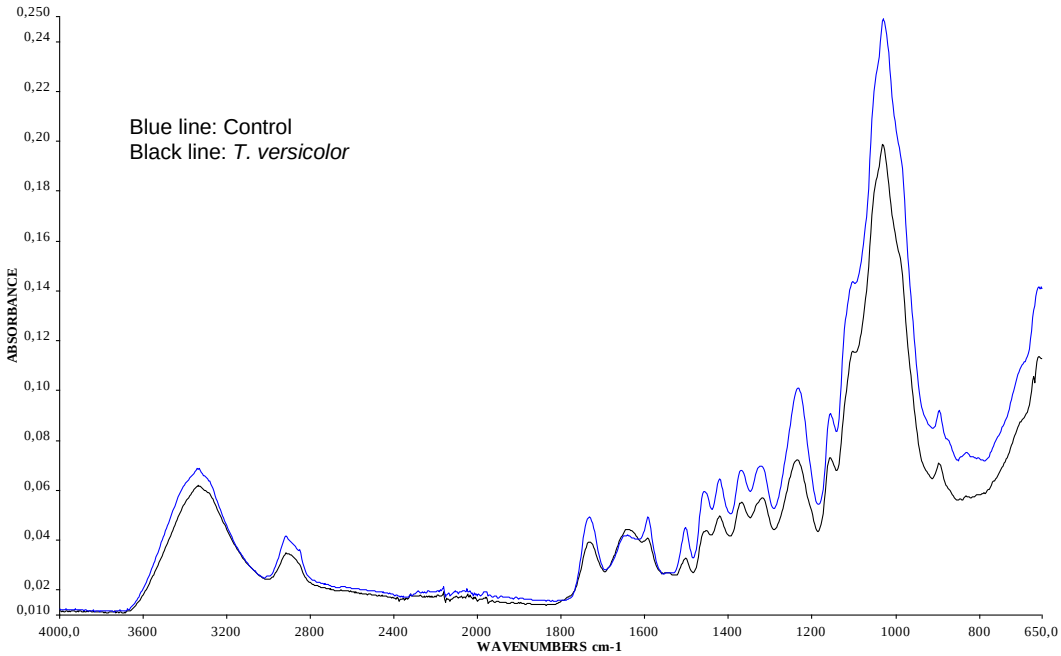

Fig. 4a. IR spectra of specimen decayed by *T. versicolor* and control specimen

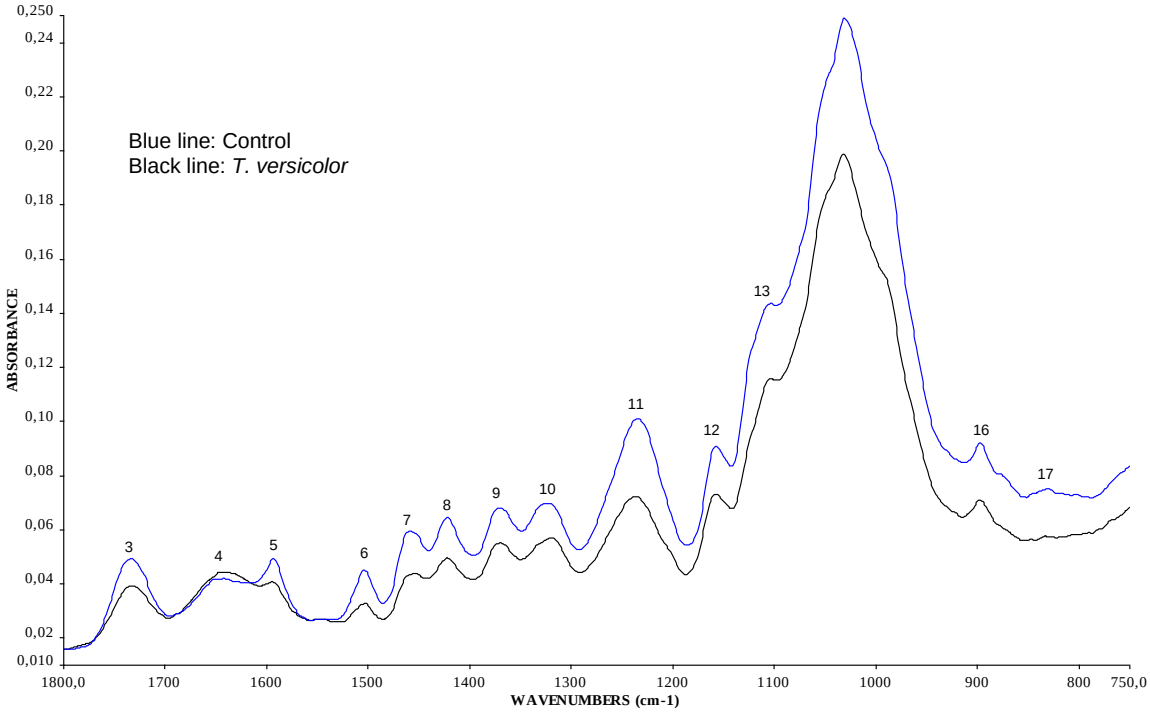

Fig. 4b. IR bands of *T. versicolor* and control specimens in the range of 1800 to 750 cm^{-1}

A remarkable increase in intensity that was observed at the 1648 cm^{-1} (4) band, originating from lignin, can be referred to both the decrease in intensity at the 1593 cm^{-1} (5) band and the structural change in lignin during *T. versicolor* degradation. These findings were compatible with the results from a study by Faix *et al.* (1991). According to their results, beech wood degraded by white-rot fungi displayed an increased intensity of the 1646 cm^{-1} band while the band at 1596 and 1506 cm^{-1} showed a decreased intensity (Faix *et al.* 1991). Furthermore, the band at 830 cm^{-1} (17) from syringyl lignin was nearly absent in the specimen degraded by *T. versicolor*. The spectra of the degraded specimen by *T. versicolor* displayed lower absorbance compared to the control specimen in the peak at the wave number 1456 cm^{-1} (7) related to the polysaccharides. Even though the mass losses were relatively low in the specimen degraded by *T. versicolor* compared to *T. palustris* and *G. trabeum* (Terzi *et al.* 2012), small changes were observed in polysaccharides' band intensities compared to *T. palustris* and *G. trabeum*. Thus, it is clear that *T. versicolor* degraded mostly lignin and also a small amount of carbohydrates, while *T. palustris* and *G. trabeum* selectively degraded the polysaccharides of the wood. As expected, smaller changes were observed in the polysaccharide band intensities of the decayed specimen by *T. versicolor* compared to *T. palustris* and *G. trabeum* degradation. This result is also compatible with the relatively low mass losses in the specimen (Terzi *et al*. 2012). Remarkable differences occurred in the degradation of the lignin in the specimen degraded by *T. versicolor*. According to the ATR spectroscopy results, decreases and modifications in the lignin bands were more significant compared to polysaccharides' absorption bands.

Anatomical Observations

Microscopic investigations performed on the deteriorated heartwood samples of *L. orientalis* by white-rot and brown-rot fungi were evaluated separately. Images of the control sample are shown in Fig. 5 for comparisons.

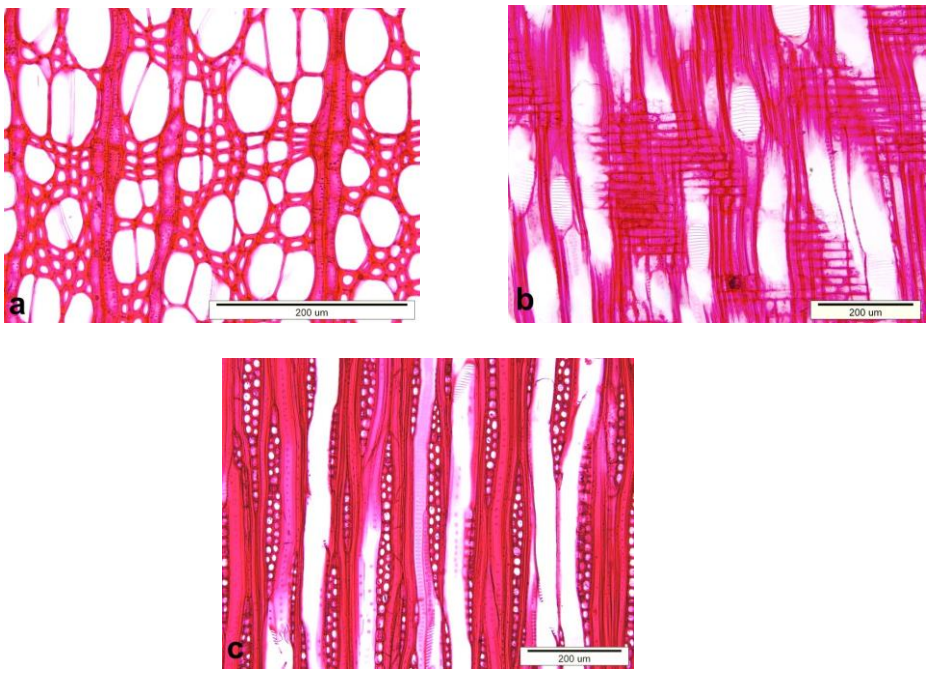

Fig. 5. Light micrographs of control: a) Cross section, b) Radial section, c) Tangential section.

The heartwood is basically reddish brown to brown. The sapwood color is distinct from the heartwood color and it has a distinctive sapwood border. Since the growth rings are marked by a few rows of radially flattened fibers, the growth ring boundaries are distinct. The wood is diffuse-porous and the vessels are mostly solitary, rarely in short (2-3 vessels) radial rows. The shapes of the solitary vessels are slightly angular in their outline. The number of vessels/mm² are 49 to 65. The mean tangential vessel diameter is 66 to 56 µm. The mean vessel element length is 775 µm. Inter-vessel pits are scalariform. Vessel-ray pits with much reduced borders are apparently simple: pits vary from horizontal (scalariform, gash-like) to vertical (palisade). Rays are 1-3(-6)-seriate, and body ray cells are procumbent with mostly 1 to 4 rows of upright and / or square marginal cells. The traumatic axial canals are sometimes present in long tangential lines (Efe 1987; Bozkurt *et al.* 1989; Wheeler *et al.* 2010).

Anatomical changes in the decayed wood by the white-rot fungus, Trametes versicolor

Figure 6 (in multiple parts) shows samples exposed to fungal decay.

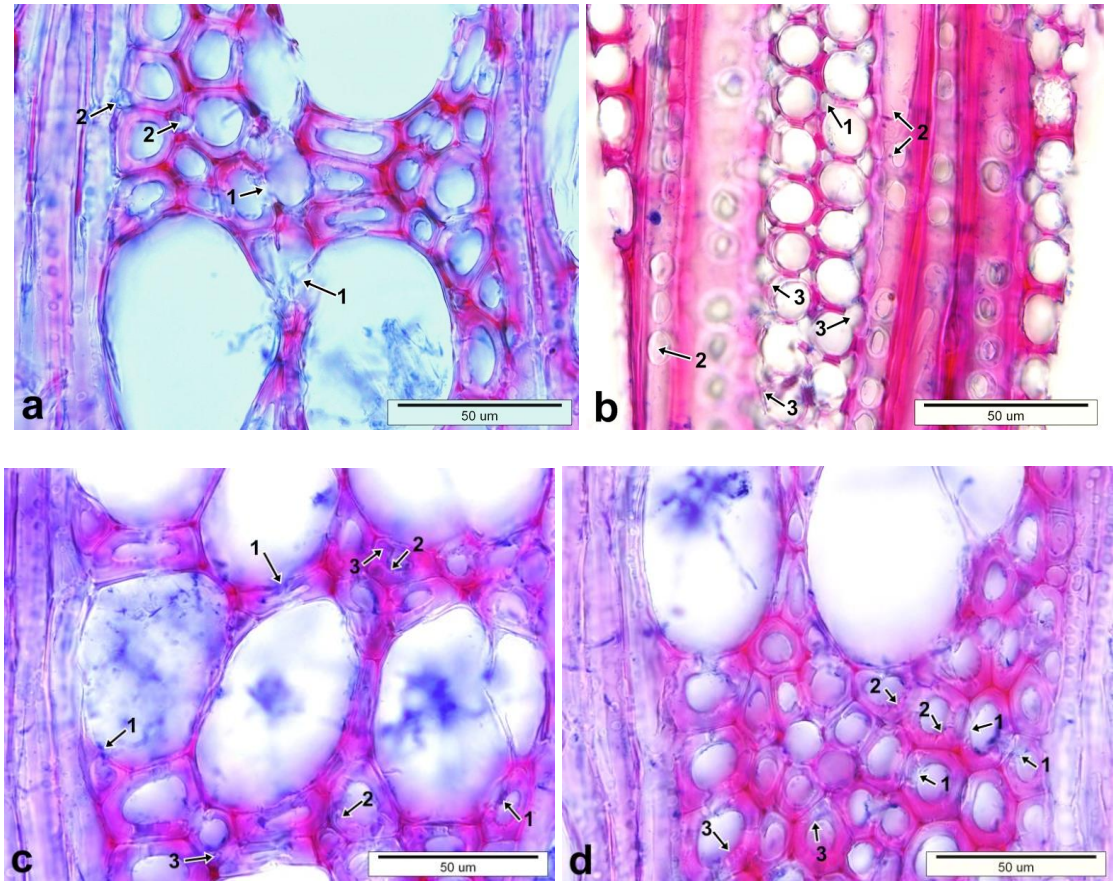

Fig. 6. (*T. versicolor* attack). a) Fungal attack from the lumina (arrows 1) and from the cell corners of fibers (arrows 2), b) Fungal attack from the cell corners of ray parenchyma (arrows 1), bore holes composed due to the progressing of pit erosion (arrows 2), and the separations in the ray parenchyma cells indicating selective degradation (arrows 3), c) Hyphae boring the cell walls (arrows 1), dentate structure in fiber cell walls indicating irregular degradation (arrows 2), and splits in the fiber cell walls (arrows 3), d) General thinning in the secondary walls of fiber cells (arrows 1), dentate structure in fiber cell walls (arrows 3), and minute cracks in the secondary walls of fiber cells (arrows 2)

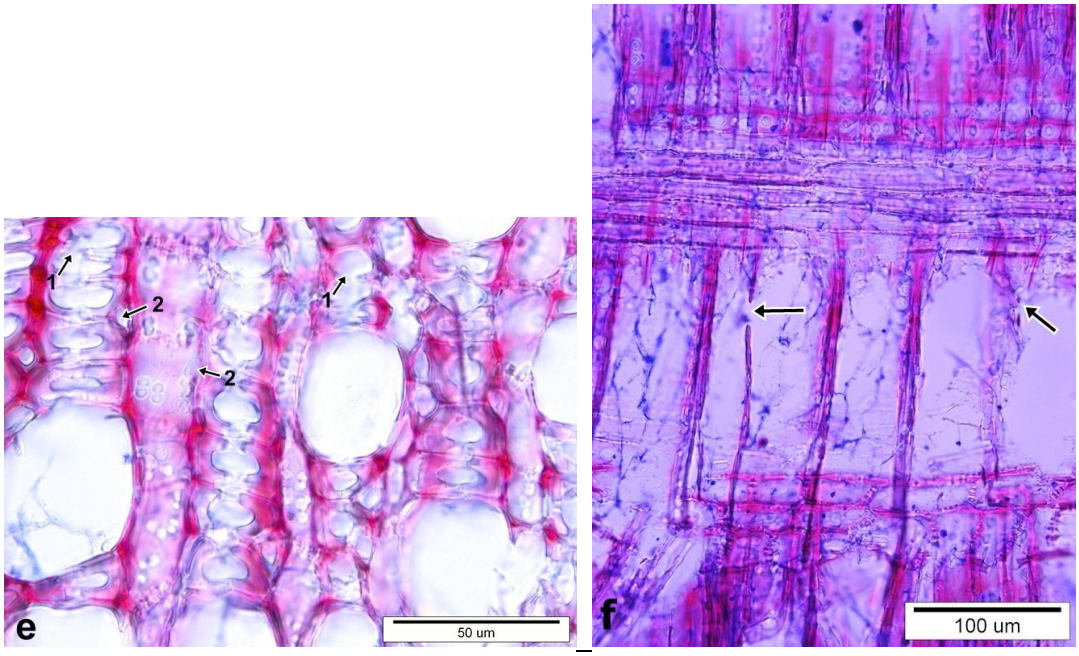

Fig. 6. (continued). e) Local degradation resulting in the localized removal of the fiber cell walls and middle lamella (arrows 1), separations between fiber-ray parenchyma cells in less quantity (arrows 2), f) Local degradation resulting in the localized removal of the fiber cell walls and middle lamella (arrows)

After 12 weeks of an incubation period, selective and simultaneous white-rot decay was found in the wood specimens. The attack of *T. versicolor* in the cell walls was observed both from the lumina and from the cell corners (Fig. 6a and Fig. 6b). Fungal attack from the cell corners was detected particularly in the ray parenchyma cells (Fig. 6b). Hyphae boring the cell walls were also seen (Fig. 6c). This morphological alteration has been attributed in the literature to the interference of extractives (Lee *et al.* 2009). That type of fungal attack resulted in cell wall thinning from the lumen outwards.

Two types of cell wall thinning were observed in the microscopic sections; one was characterized by the general erosion of the cell walls adjacent to the hyphae growing in the lumen surface (Fig. 6d), and the other one was a local degradation resulting from the localized removal of the cell walls and middle lamella (Fig. 6e and Fig. 6f). General thinning in the fiber cell walls showed a dentate structure, indicating irregular degradation (Fig. 6c and Fig. 6d). Although, the fiber cell wall thinning was extensive in some parts of sections, the middle lamellae and the cell corners were much more resistant to decomposition. Minute cracks in large quantities were detected in the secondary cell walls of the fibers (Fig. 6d). However, splits in the cell walls were rarely seen (Fig. 6c). Erosion of the simple and bordered pits caused round or oval openings (Fig. 6g). Bore holes composed due to the progressing of pit erosion were detected (Fig. 6b and Fig. 6g). In the longitudinal sections, erosion channels appeared with U-shaped notches (Fig. 6h). All of the changes in the anatomical structure of the wood mentioned above were interpreted as simultaneous degradation. It has been reported that the presence of cell wall thinning, minute cracks in the cell walls, rounded or oval pit erosions, bore holes, and erosion channels indicate simultaneous degradation (Wilcox 1968; Liese 1970; Highley and Murmanis 1987; Schwarze 1995; Anagnost 1998; Luna *et al.* 2004).

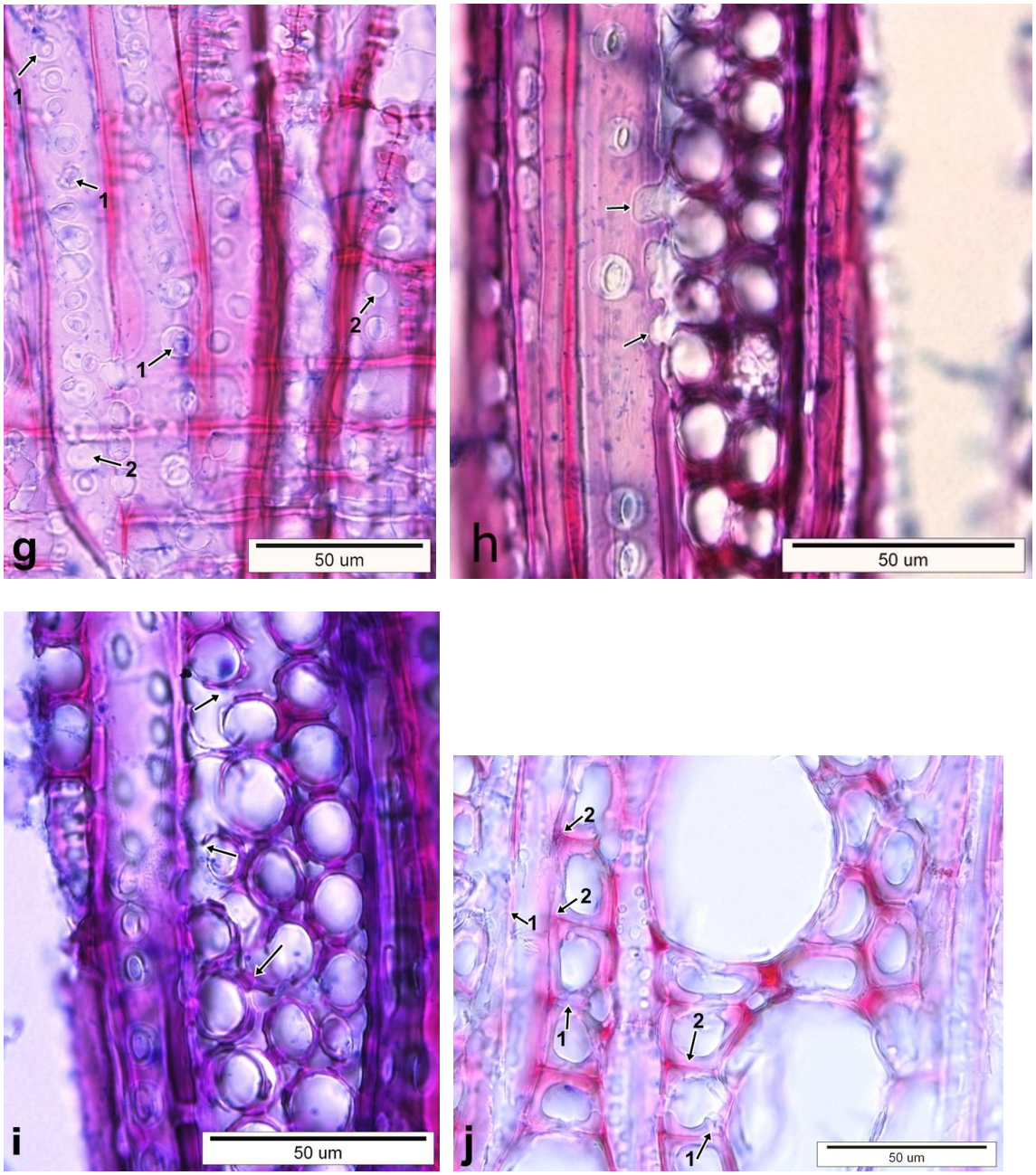

Fig. 6 (continued). g) Round or oval openings in pits (arrows 1), bore holes composed due to the progressing of pit erosion (arrows 2), h) Erosion channel with U-shaped notches (arrows), i) Separations in the ray parenchyma cells indicating selective degradation (arrows), j) Lighter color areas in the middle lamella (arrows 1) and in the secondary cell walls (arrows 2) reflect the occurrence of selective delignification.

Some clues supporting selective degradation were also found. Cell separations were evaluated as one of the most important pieces of evidence for selective degradation. Those separations in connection with the degradation of the middle lamella were clear in ray parenchyma cells (Fig. 6b and Fig. 6i). On the other hand, separations were observed in less quantity both between the fiber cells and the fiber-ray parenchyma cells (Fig. 6a

and Fig. 6e). The middle lamella of the wood cells stained with safranin showed lighter areas reflecting the occurrence of selective delignification (Fig. 6j). Those areas were also observed in the secondary walls of the wood cells.

Schwarze (2007) noticed that lignin was first removed from the secondary wall nearest the lumen and then throughout the secondary wall toward the middle lamella in selective degradation. The middle lamella and cell corners were the last areas to be degraded. Schwarze (2007) also reported that parenchyma cells were often preferentially degraded by white-rot fungi causing a selective delignification. Although observations were not performed on different stages of decomposition, the results of the current study can be considered to be compatible with the results of Schwarze (2007).

Obst *et al*. **(**1994) studied the degraded sapwood blocks of seven hardwood species including sweetgum (*L. styraciflua* L.) by *T. versicolor*. Their results showed that after 6 weeks of decay, the fiber cell walls were degraded preferentially to the cell corners, middle lamellae, vessels, and ray parenchyma cells. Vessels and ray parenchyma cells were rapidly colonized by fungal hyphae but were resistant to decay in a high degree compared to the fiber cells.

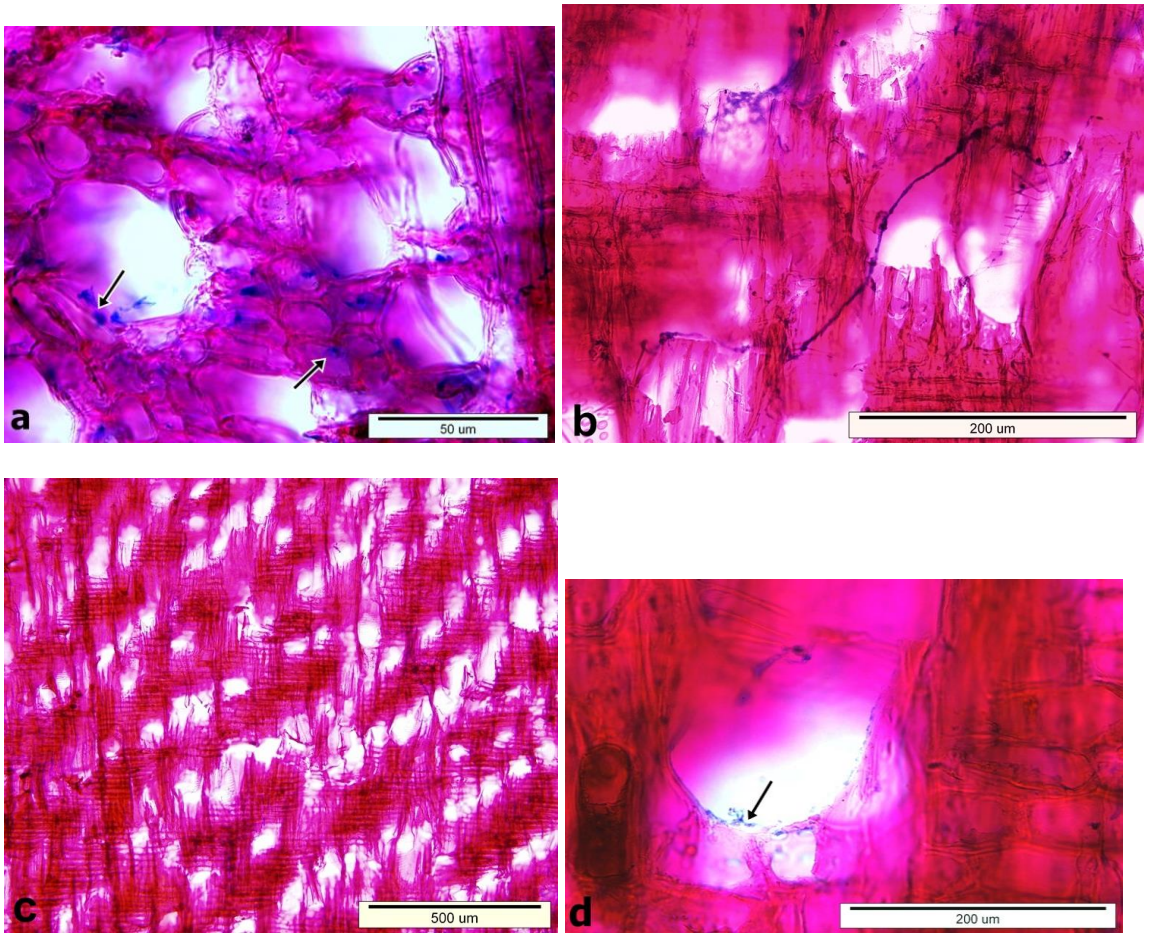

Fig. 7. (*T. palustris* attack). a) Destruction in the wood structure, hyphae on the surface of S_3 layer in the lumen side (arrows), b-c) Destruction in the wood structure, d) Hyphae on the surface of S_3 layer in the lumen side (arrow)

Since in the current study, the microscopic investigations were not realized in the specimens decayed at weekly intervals, as had been done in most of the previous studies, it is difficult to state which types of wood cells were degraded preferentially. On the other hand, the cell corners and middle lamella of the fiber cells can be considered much more resistant to decay when compared with the ray parenchyma cells.

Highley and Murmanis (1987) reported that *T. versicolor* severely degraded the middle lamella and the cell corners of sweetgum (*L. styraciflua* L.) without significant degradation of the adjacent cell walls. Therefore, *T. versicolor* was considered as a nonselective white-rot fungus in that study. There are also some studies that reported that *T. versicolor* is a nonselective white rotter, since it degrades carbohydrates and lignin more or less uniformly (Cowling 1961; Liese 1970; Anagnost 1998). Since the degraded middle lamella and cell corners of the ray parenchyma cells showed significant degradation together with the adjacent cell walls in the current study, it was considered selective degradation.

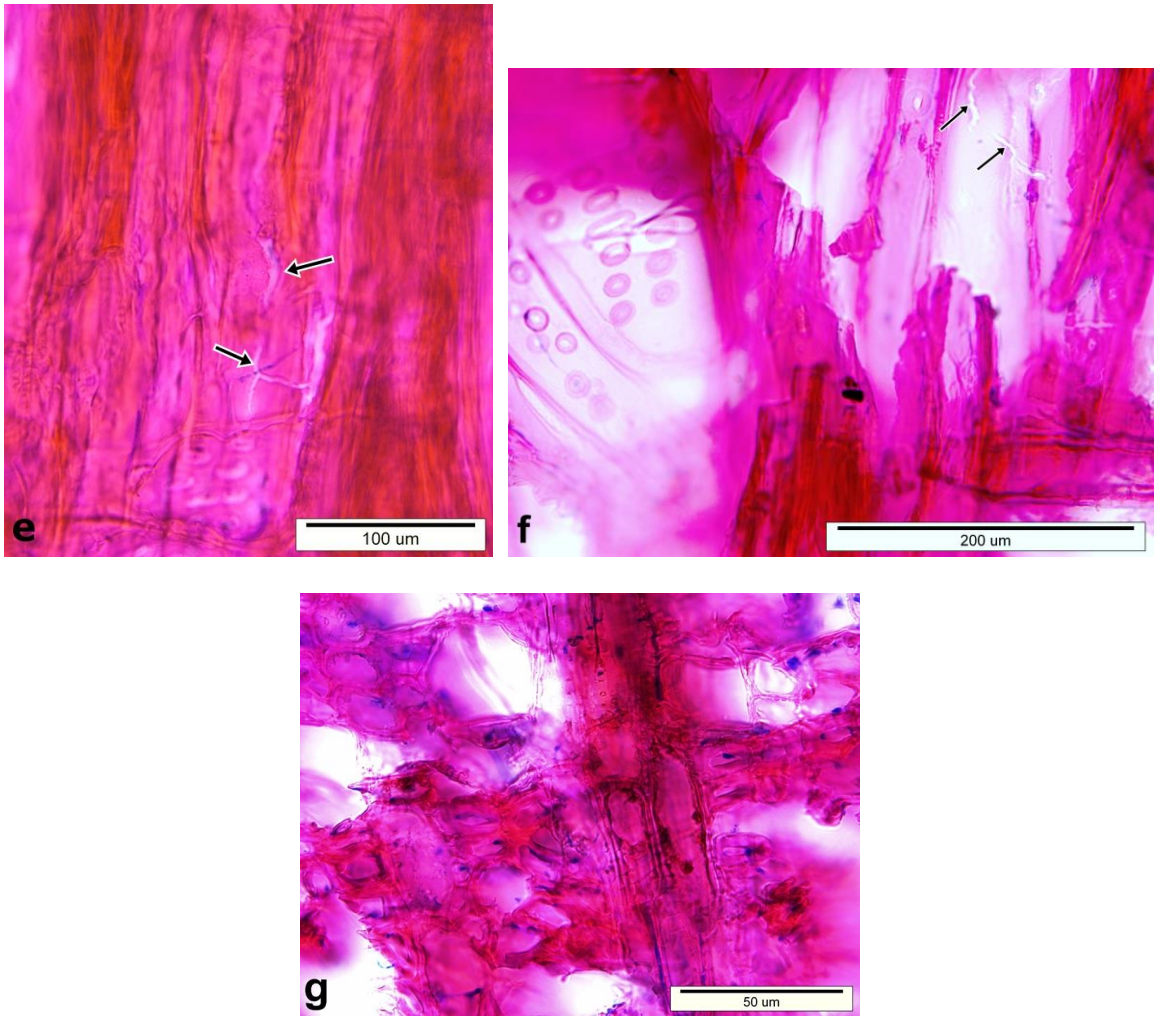

Fig. 7. (continued). e) Cracks in the cell walls (arrows), loose structure in the all cell walls, f) Cracks in the cell walls (arrows), g) Loose structure in the all cell walls

Anatomical changes in decayed wood by the brown-rot fungus, Tyromyces palustris

A great amount of destruction was observed in the wood structure. It is thought that the cell collapse caused destruction because there was a distortion in the plane of wood cells (Fig. 7a,b,c). Extensive degradation in all types of cell walls was also observed. Most of the hyphae were seen on the surface of the S_3 layers in the lumen side (Fig. 7a and Fig. 7d). Cracks in the cell walls were detected, whilst no erosion channels and distinct boreholes were observed (Fig. 7e,f). Almost all of the cell walls showed a loose structure (Fig. 7e,g), and they were in an expanded form. There is an assumption about the penetration of cellulose degrading enzymes into the cell walls stating that the enzymes cannot penetrate without any loosening of the cell wall matrix (Cowling and Kirk 1976; Hill and Papadopoulos 2001).

Some studies have been reported that parenchyma cells are resistant to brown-rot decay (Worrall *et al.* 1997; Schwarze *et al.* 2000; Schwarze *et al.* 2003). However, the results of the current study showed almost the same degree of decomposition in all of the types of cell walls.

CONCLUSIONS

1. Twenty-six extracts were identified in the ethanol/toluene extraction and 17 extracts were identified from the ethanol extraction. There were 13 main extractives listed in the table (peak area above 1%) for this study. The extractives identified in the heartwood of *L. orientalis* are known for contributing to biological activity. Individual chemicals found in *L. orientalis* heartwood extracts have been shown in the literature to have more of an impact on biological activity.
2. There was a morphological alteration occurring where the hyphae were boring the cell wall during the white-rot degredation. According to the literature, this observation is due to an interference of the extractives. More investigations are needed to determine whether the extractives play a role in this observation.
3. The microscopy examinations demonstrated that *T. versicolor* primarily degraded lignin and carbohydrates simultaneously, but it was also observed that in some sections the lignin was degraded preferentially. As expected, less changes were observed in the polysaccharide FT-IR band intensities of the decayed specimen by *T. versicolor* compared to *T. palustris* and *G. trabeum* degradation, which was compatible with relatively low mass losses in the specimen.
4. ATR spectroscopy examinations also supported that the degree of lignin degradation was higher than hemicellulose degradation, while cellulose showed no deterioration after 12 weeks of *T. versicolor* degradation.
5. A great amount of destruction and extensive degradation in all types of cell walls were observed in the wood structure during the brown rot decay. During the brown rot decay, polysaccharides were extensively depolymerized and removed, and although the lignin may also have been modified, its residue largely remained behind. This was verified by both the Klason lignin determination and FT-IR ATR spectroscopy observations.
6. The remarkable increase in the hot alkali solubility value in the specimen exposed to *T. palustris* indicated the decomposition and removal of polysaccharides. This

was also compatible with the FT-IR ATR spectroscopy results, indicating a significant decrease in the intensities of the bands at 1734 cm^{-1}, 1372 cm^{-1}, 1157 cm^{-1}, and 896 cm^{-1}. It was clear that *T. palustris* and *G. trabeum* caused a remarkable degradation of polysaccharide structure of wood and also caused some modifications in the lignin structure.

ACKNOWLEDGEMENTS

Decayed test specimens were obtained from our previous study supported by the Coordination Unit for Scientific Research Projects, Istanbul University, Turkey (Project No: 4436).

REFERENCES CITED

American Society for Testing Materials (ASTM). (2010). *Annual Book of ASTM Standards*, Vol. 04.10. ASTM, West Conshohocken, Pennsylvania, USA.

American Wood Protection Association (AWPA) (2010). *Annual Book of AWPA Standards*, AWPA Birmingham, Alabama, USA.

Anagnost, S.E. (1998). "Light microscopic diagnosis of wood decay," *IAWA Journal* 19(2), 141-167.

Bozkurt, A. Y., Göker, Y., and Kurtoğlu, A. (1989). "Sığla ağacının bazı özellikleri," *İstanbul Üniversitesi Orman Fakültesi Dergisi* Seri B 39(1), 43-52 (in Turkish).

Blanchette, R. A. (1995). "Degradation of the lignocellulosic complex in wood," *Canadian Journal of Botany* 73 (Suppl.), S999-S1010.

Cowling, E. B. (1961). "Comparative biochemistry of the decay of sweetgum sapwood by white-rot and brown-rot fungi," *U.S. Dep. Agric. Tech. Bull*. No. 1258, 1-75.

Cowling, E. B., and Kirk, T. K. (1976). "Properties of cellulose and lignocellulosic materials as substrates for enzyme conversion processes," *Biotechnology and Bioengineering Symposium* 6, 95-124.

Davis, M. W. (1998). "A rapid modified method for compositional carbohydrate analysis of lignocellulosics by high pH anion exchange chromatography with pulsed amperometric detection (HPAEC/PAD)," *Journal of Wood Chemistry* and Technology 18, 235-252.

Efe, A. (1987). "*Liquidambar orientalis* Mill. (Sığla ağacı)'in morfolojik ve palinolojik özellikleri üzerine araştırmalar," *İstanbul Üniversitesi Orman Fakültesi Dergisi* Seri A, 37(2), 84-114 (in Turkish).

Eriksson, K. E. L., Blanchette, R. A., and Ander, P. (1990). *Microbial and Enzymatic Degradation of Wood and Wood Components*, Springer-Verlag, Berlin, Heidelberg, New York.

Faix, O. (1991). "Classification of lignins from different botanical origins by FTIR spectroscopy," *Holzforschung* 45, 21-27.

Faix, O., Bremer, J., Schmidt, O., and Stevanovic, T. (1991). "Monitoring of chemical changes in white-rot degraded beech wood by pyrolysis-gas chromatography and Fourier transform infrared spectroscopy," *Journal of Analytical and Applied Pyrolysis* 21, 147-162.

Flournoy, D. S., Kirk, K. T. and Higley, T. L. (1991). "Wood decay by brown rot fungi: Changes in pore structure and cell wall volume," *Holzforschung* 45, 383-388.

Harrington, K. J, Higgins, H. G., and Michell, A. J. (1964). "Infrared spectra of *Eucalyptus regnans* F. Muell. and *Pinus radiata* D. Don.," *Holzforschung* 18, 108-113.

Hafizoglu, H., Reunanen, M., and Istek, A. (1996). "Chemical constituents of balsam from *Liquidambar orientalis*," *Holzforschung* 50, 116-117.

Hatakka, A., and Hammel, K. E. (2010). "Fungal biodegradation of lignocelluloses," In: *The Mycota*, 2nd Edition, Vol. X, *Industrial Applications*, M. Hofrichter (ed.), Springer-Verlag, Berlin, Heidelberg.

Higgins, H. G., Stewart, C. M., and Harrington, K. J. (1961). "Infrared spectra of cellulose and related polysaccharides," *J. Polymer Sci*.51 (155), 59-84.

Highley, T. L. and Murmanis, L. L. (1987). "Micromorphology of degradation in western hemlock and sweetgum by the white-rot fungus *Coriolus versicolor*," *Holzforschung* 41, 67-71.

Hill, C. A. S., and Papadopoulos, A. N. (2001). "A review of methods used to determine the size of the cell wall microvoids of wood," *Journal of the Institute of Wood Science* 15, 337-345.

Lee, Y. S., Kim, J., Lee, S. G., Oh, E., Shin, S. C., and Park, I. K. (2009). "Effects of plant essential oils and components from Oriental sweetgum (*Liquidambar orientalis*) on growth and morphogenesis of three phytopathogenic fungi," *Pesticide Biochemistry and Physiology* 93, 138-143.

Liese, W. (1970). "Ultrastructural aspects of woody tissues disintegration," *Annual Review of Phytopathology* 8, 231-258.

Luna, M. L., Murace, M. A., Keil, G. D., and Otano, M. E. (2004). "Patterns of decay caused by *Pycnoporus sanguineus* and *Ganoderma lucidum* (Aphyllophorales) in poplar wood," *IAWA Journal* 25 (4), 425-433.

Mohebby, B. (2005). "Attenuated total reflection infrared spectroscopy of white-rot decayed beech wood," *International Biodeterioration & Biodegradation* 55, 247-251.

Naumann, A., Gonzales, M. N., Peddireddi, S., Kues, U., and Polle, A. (2005). "Fourier transform infrared microscopy and imaging: Detection of fungi in wood," *Fungal Genetics and Biology* 42, 829-835.

Nuopponen, M. H., Wikberg, H. I., Birch, G. M., Jaaskelainen, A. S., Maunu, S. L., Vuorinen, T., and Stewart, D. (2006)."Characterization of 25 tropical hardwoods with Fourier transform infrared, ultraviolet resonance Raman, and ^{13}C-NMR cross-polarization / magic-anglespinning spectroscopy," *Journal of Applied Polymer Science* 102, 810-819.

Obst, J. R., Highley, T. L., and Miller, R. B. (1994). "Influence of lignin type on the decay of woody angiosperms by *Trametes versicolor*," *Biodeterioration Research 4*, G. C. Liewellyn, *et al*. (eds.), Plenum Press, New York.

Pandey, K. K. (1999). "A study of chemical structure of soft and hardwood and wood polymers by FTIR spectroscopy," *Journal of Applied Polymer Science* 71, 1969-1975.

Pandey, K. K., and Pitman, A. J. (2003). "FTIR studies of the changes in wood chemistry following decay by brown-rot and white-rot fungi," *International Biodeterioration & Biodegradation* 52, 151-160.

Pandey, K. K., and Pitman, A. J. (2004). "Examination of the lignin content in a softwood and a hardwood decayed by a brown-rot fungus with the acetyl bromide

method and Fourier transform infrared spectroscopy," *Journal of Polymer Science*: *Part A: Polymer Chemistry* 42, 2340-2346.

Rumana, R., Heyser, R. L., Finkeldey, R., and Polle, A. (2010). "FTIR spectroscopy, chemical and histochemical characterization of wood and lignin of five tropical timber wood species of the family of Dipterocarpaceae," *Wood Sci. Technol.* 44, 225-242.

Runkel, R. O. H., and Wilke, K. D. (1951). "Zur Kenntnis des thermoplastischen Verhaltens von Holz. II. Mittl.," *Holz Roh Werkst.* 9, 260-270.

Schwarze, F. W. M. R. (1995). "Entwicklung und biomechanische Auswirkungen von holzzersetzenden Pilzen in lebenden Bäumen und *in vitro*," PhD thesis, University of Freiburg, Germany.

Schwarze, F. W. M. R., Baum, S., and Fink, S. (2000). "Dual modes of degradation by *Fistulina hepatica* in xylem cell walls of *Quercus robur*," *Mycological Research* 104, 846-852.

Schwarze, F. W. M. R, Fink, S., and Deflorio, G. (2003). "Resistance of parenchyma cells in wood to degradation by brown rot fungi," *Mycological Progress* 2(4), 267-274.

Schwarze, F. W. M. R. (2007). "Wood decay under the microscope," *Fungal Biology Reviews* 21, 133-170.

TAPPI (1999). T-257 cm-85: "Sampling and preparing wood for analysis," TAPPI Test Methods, TAPPI Press, Atlanta Georgia, USA.

TAPPI (1999). T 211 om-93. "Ash in wood, pulp, paper and paperboard: Combustion at 525°C," TAPPI Test Methods, TAPPI Press, Atlanta Georgia, USA.

TAPPI (1999). T 207 om-93. "Water solubility of wood and pulp," TAPPI Test Methods, TAPPI Press, Atlanta Georgia, USA.

TAPPI (1999). T 212 om-98. "One percent sodium hydroxide solubility of wood and pulp," TAPPI Test Methods, TAPPI Press, Atlanta Georgia, USA.

TAPPI (1987). T 204 om-88. "Solvent extractives of wood and pulp". TAPPI Test Methods, TAPPI Press, Atlanta Georgia, USA.

Terzi, E., Kartal, S. N., Ibanez, C. M., Kose, C., Arango, R., Clausen, C. A., and Green, III, F. (2012). "Biological performance of *Liquidambar orientalis* Mill. Heartwood," *International Biodeterioration and Biodegradation* 75, 104-108.

Wheeler, E. A., Lee, S. J., and Baas, P. (2010). "Wood anatomy of the *Altingiaceae* and *Hamamelidaceae*," *IAWA Journal* 31(4), 399-423.

Wilcox, W. W. (1968). "Changes in wood microstructures through progressive stages of decay," *Res. Pap. FPL 70*. U.S. Department of Agriculture, Forest Serv., Forest Products Lab., Madison, WI, 46.

Winandy, J. E. and Morrell, J. J. (1993). "Relationship between incipient decay, strength, and chemical composition of Douglas-Fir heartwood," *Wood and Fiber Science* 25(3), 278-288.

Worrall, J. J., Anagnost, S. E., and Zabel, R. A. (1997). "Comparison of wood decay among diverse lignocolous fungi," *Mycologia* 89 (2), 199-219.

Article submitted: March 13, 2013; Peer review completed: April 9, 2013; Revised version received and accepted: April 18, 2013; Published: April 23, 2013.